Journal of Engineering and Technology for Industrial Applications

ISSN ONLINE: 2447-0228

ITEGAM-JETIA

Manaus, v.12 n.57, p. 176-187. January/February, 2026.

DOI: https://doi.org/10.5935/jetia. v12i57.2851

RESEARCH ARTICLE OPEN ACCESS

INFLUENCE OF DEFECTS ON THE MECHANICAL PROPERTIES OF METALLIC COATINGS OBTAINED BY THERMAL SPRAYING: A REVIEW

Uirá Rodrigues da Silveira Montani[1], Marília Garcia Diniz[2]
Paolo Bettini[3] and Hector Reynaldo Meneses Costa[4]

[1]Programa de Pós-Graduação em Engenharia Mecânica e dos Materiais do Centro Federal de Educação Tecnológica Celso Suckow da Fonseca (PPEMM - CEFET-RJ), Rio de Janeiro, Brazil
[2]Programa de Pós-Graduação em Engenharia Mecânica da Universidade do Estado do Rio de Janeiro (PPGEM – UERJ), Rio de Janeiro, Brazil
[3, 4]Aerospace Science and Technology Department of Politecnico Di Milano, Milan, Italy.

[1]https://orcid.org/0009-0005-8174-9164, [2]https://orcid.org/0000-0002-1836-8618
[3]https://orcid.org/0000-0003-1083-5792, [4]https://orcid.org/0000-0002-0887-6838

Email: uirarsilveira@yahoo.com.br, mgarciadiniz@gmail.com, paolo.bettini@polimi.it, hectorey@gmail.com

ARTICLE INFO

Article History
Received: October 24, 2025
Revised: November 20, 2025
Accepted: January 1, 2026
Published: January 31, 2026

Keywords:
Coatings,
Thermal Spray,
Defects,
Machine Learning

ABSTRACT

Thermally sprayed coatings are used as superior engineering materials, to prolong the service life of components and reduce manufacturing costs, but also significantly saving limited resources and energy, a technique capable to protect surfaces from erosive wear, corrosion, and enhance the tribological properties of a broad range of engineering materials. The study outlines the technological principle and process of thermal spray technique, and explores microstructural defects of thermal sprayed coatings, including pores, microcracks, unmelted particles, and oxides, exploring their formation mechanisms and effects. This paper also explores machine learning as a valuable tool that enables more accurate prediction of defect formation and supports the development of optimized spraying parameters.

I. INTRODUCTION

Thermal spray coatings are widely applied in engines, pumps, compressors, pipelines, and medical implants, providing cost-effective and reliable means to protect, repair, and extend component lifespan. However, inherent defects arise from compositional imbalances and surface irregularities generated during the layer-by-layer deposition process, leading to stress concentration and crack formation. These defects, influenced by the feedstock material and deposition parameters, reduce coating density and compactness, thereby impairing oxidation resistance and overall performance. This paper aims to present a comprehensive review of the current state of thermal spraying, beginning with an overview of existing technologies and recent advancements, followed by a detailed analysis of the main defects observed in such coatings. It also discusses current challenges in the field and identifies key research gaps, contributing to a deeper understanding and guiding future investigations in thermal spray technology.

II. METHODOLOGY

The literature survey was conducted as part of the development of this research paper. This study examined different thermal spray processes and the formation of defects on the surface and within the core of metallic and ceramic coatings. The literature review provides a strong foundation for the current research and highlights its relevance for future investigations. The study relied on references from various national and international journals, articles, and reputable websites.

III. LITERATURE REVIEW

III.1 THERMAL SPRAY

The thermal spray process (TS) involves several distinct deposition techniques utilizing a concentrated heat source to liquefy different material compounds. These molten particles are then propelled onto the surface to be coated, each carrying different levels of kinetic energy [1]. The particles coalesce into microstructural artifacts resembling splats, which solidify into an interconnected network of a lamellar microstructure, typically resulting in a functional coating ranging from 50 µm to several millimeters in thickness [1-5] (see Figure 1). The thermal spray technique is a surface modification process that enhances the substrate material characteristics, cappable of supplying the underlying substrate with good thermal insulation, thermally stable, wear resistant, high temperature oxidation resistant and hard coating [2-4]. Rigamonti et al. [5] proposed a method for embedding polymer-coated optical fibers with inscribed fiber Bragg gratings (FBGs) onto steel substrates using the thermal spray technique. This approach ensured strong adhesion, efficient strain transfer, and minimal invasiveness, while preserving the integrity of the fiber's core and cladding. The thermal spray process, performed at low temperatures, enabled the integration of the fiber into the metallic structure without causing damage, and the resulting metal layer provided additional mechanical protection, allowing the system to be used in harsh environments characterized by severe corrosion and wear.

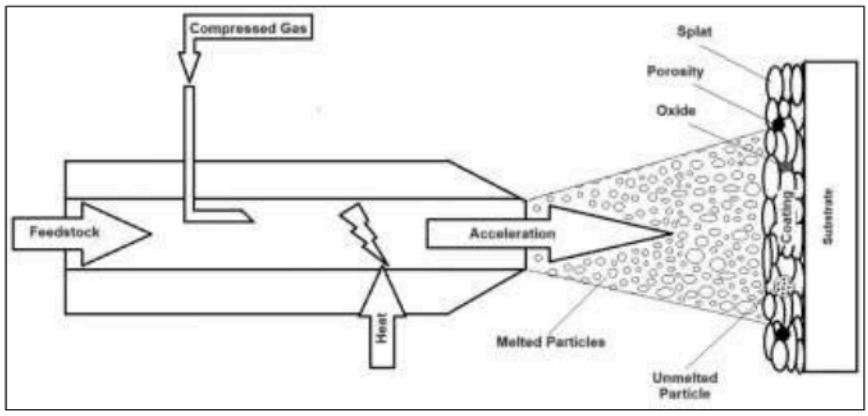

Figure 1: Thermal Spray Process.
Source: Authors, (2026).

Thermal spray processes are typically grouped according to their energy source, as illustrated in Figure. 2. These processes are differentiated based on the temperature and velocity of the jet stream they generate. Splats are frequently observed in thermally sprayed coatings, with the characteristics of splat boundaries (often oxides at these interfaces), porosity, and residual stress varying significantly. Moreover, corrosive substances can exploit the interplat bonding and interconnected pores as pathways for short-circuit diffusion [4].

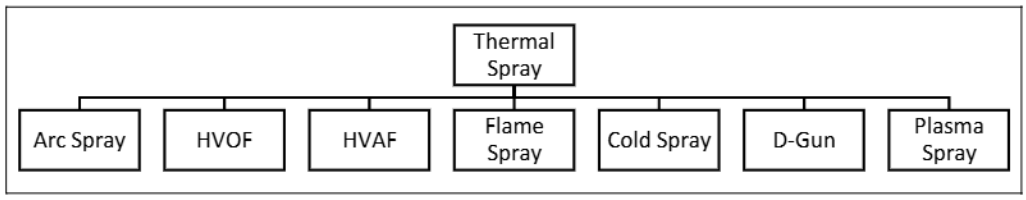

Figure 2: Generalized classification of thermal spray techniques.
Source: Authors, (2026).

Surface modifications using coating technologies serve to safeguard the substrate material, diminishing replacement expenses by slowing down material degradation, consequently prolonging the lifespan of components [1],[2]. Coating methods are categorized based on specific needs, including desired coating thickness, adhesion mechanism, necessary mechanical strength, component geometry and chemistry, coating process conditions suitable for the component, and the operating conditions of the coating [2]. Thermal spray processes have been extensively validated across industries such as steel, power generation, automotive, aerospace, marine, and petrochemical sectors for safeguarding and repairing components [4-7]. Utilizing thermal spray for repairing and remanufacturing components with localized defects or failures not only extends their service life but also proves to be cost-effective. This approach significantly conserves resources and energy, aligning well with the core principles of sustainable development [6]. The metallic coatings manufactured through additive manufacturing (AM) processes, such as thermal spray, often exhibit irregular surface morphology compared to those produced by conventional methods.

These irregularities stem from the layer-by-layer deposition and fusion occurring on the material surfaces [8], [9]. Several factors contribute to the irregularity of these surfaces, including the staircase effect, agglomeration of partially fused material, spattering, splashed particles (evaporation and balling effect), and the instability of the molten pool (wetting effect). These features formed on the surfaces act as stress concentration sites, facilitating crack formation. Furthermore, the size of the feedstock and deposition parameters also influence the surface morphology of the coatings [9],[10]. Typically, metallic alloys are not thermodynamically stable; compositional imbalances arise due to metallurgical transformations occurring in the structures, retaining crystallographic imperfections or defects [8],[11]. The commonly found defects in single-material-printed parts are microcracks, porosity, unmelted or solidified particles. Bonding defects arise from inadequate energy input, potentially leading to pore formation at the interface [8]. Cavities and micro-cracks stem from shrinkage, whereas pores result from anomalous gas entrapment within the molten material. In cold spray additive manufacturing (AM)

processes, such as deposition, insufficient bonding between particles and inefficient plastic deformation may give rise to the formation of micro-pores and inter-particle boundaries at lower impact velocities [9]. The objective of this paper is to comprehensively review the current state of knowledge in thermal spraying. It begins by providing an overview of thermal spraying technologies, highlighting recent advancements in the field. Subsequently, it conducts an in-depth analysis of various defects encountered in thermal spray coatings. Finally, the paper addresses the current challenges and issues encountered by researchers in this domain. The authors anticipate that this manuscript will contribute significantly to the existing body of knowledge by offering a detailed examination and identification of challenges for future research endeavors.

III.2 DEFECTS IN COATINGS

III.2.1 Porosity

Porosity refers to the volume of pores relative to that of the bulk material, and its increase indicates a rise in the volume of pores within the entire structure [12]. Typically, porosity ranges between 0.1 and 15% for thermal spray coatings [13]. It is an inherent characteristic of coatings. Numerous factors contribute to the porosity features in coatings during the preparation process of thermal-spraying coatings, including the impact energy of incompletely melted particles, the solidification and shrinkage of the coating, the shielding effect caused by different spray angles, and the wide gap in droplet velocity. Additionally, entrapped gas inclusions from powder and temperature play roles in porosity characteristics in coatings, such as morphology, pore diameters, pore distributions, microcrack sizes and orientations, and lamellar splats [13],[14]. Furthermore, the types of components and bonding mechanisms impact pore distributions [4].

The temperature of incoming droplets can vary from fully molten liquid to a completely solid state, depending on the particle's temperature. Liquid droplets flow freely and cover most of the spaces. The impact velocity of solid or partially melted particles must be sufficiently high to deform plastically upon impact. Consequently, particles with higher velocities undergo greater deformation, resulting in finer void closure (as seen in Figure 3). If the impact velocity is modest, solid particles may become lodged in the coating due to subsequent particles approaching later. These unformed particles have poor adhesion and should be further apart from the underlying splat, forming voids [4],[13]. Porosity reflects the fundamental properties of the coating, and typically, lower porosity indicates better coating formation and quality properties. Excessive porosity can reduce strength, abrasion resistance, and corrosion resistance [13].

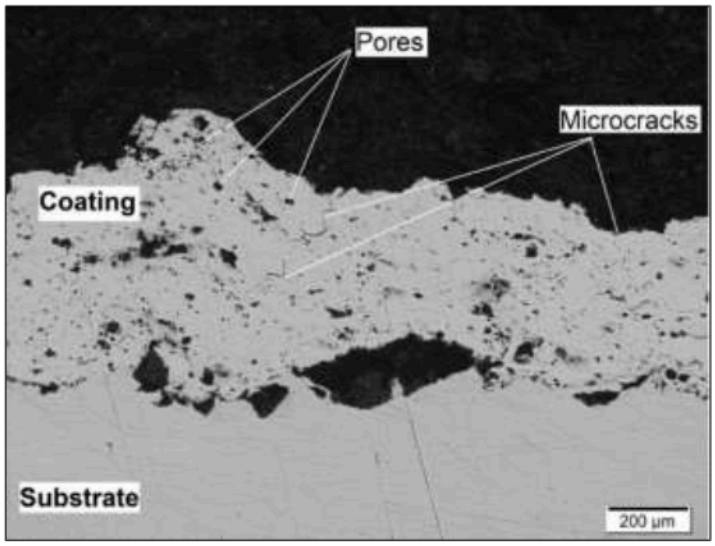

Figure 3: Cross-sectional optical micrograph of a thermal spray coating.
Source: Authors, (2026).

The temperature of incoming droplets can vary from fully molten liquid to a completely solid state, depending on the particle's temperature. Liquid droplets flow freely and cover most of the spaces. The impact velocity of solid or partially melted particles must be sufficiently high to deform plastically upon impact. Consequently, particles with higher velocities undergo greater deformation, resulting in finer void closure. If the impact velocity is modest, solid particles may become lodged in the coating due to subsequent particles approaching later. These unformed particles have poor adhesion and should be further apart from the underlying splat, forming voids [4, 13]. Porosity reflects the fundamental properties of the coating, and typically, lower porosity indicates better coating formation and quality properties. Excessive porosity can reduce strength, abrasion resistance, and corrosion resistance [13]. The pore structure plays a crucial role in determining the performance of coatings in service. Higher porosity levels can compromise certain aspects of coating performance, such as the bond strength between the coating and the substrate.

Porosity diminishes the coating's strength by promoting delamination, cracking, or spallation [13],[14], and properties like density and toughness are significantly impacted by coating porosity [15]. However, in specific scenarios, such as when aiming for coatings with reduced thermal conductivity for wear resistance, porosity might be intentionally introduced to serve as insulation within the coating. Porosity can be controlled in either case, depending on the desired coating characteristics and the appropriate process conditions [4]. According to [13] reported that the HVOF thermal spray process yields coatings with the lowest porosity among commonly used thermal spray processes. This outcome is directly attributed to the high particle velocity and low-temperature flame utilized in the process. The protective effectiveness of coatings against corrosion in various engineering materials heavily relies on coating porosity.

This is particularly critical in systems where a highly reactive (anodic) substrate requires protection from corrosion by means of a cathodic coating [15]. Porous coatings can easily be infiltrated by corrosive agents, allowing them to reach the substrate. In such cases, the coating is prone to early delamination, compromising its protective function. There are two main types of porosity: interconnected and closed (Figure 3). Each type plays a distinct role in determining the corrosion behavior of coatings. Interconnected porosity is significantly more vulnerable to corrosion compared to closed porosity because it offers direct pathways between the substrate and the corrosive environment [4]. Any porosity extending through the thickness exposes a very small anodic area to corrosion, resulting in rapid substrate corrosion due to the high corrosion current density [15]. In [16] investigated Al-5Mg alloy coatings produced via twin-wire arc thermal spray on SS400 steel substrates, employing varied spraying parameters. Porosity analysis followed the ASTM E2109-01 standard, while corrosion performance in 3.5 wt. % NaCl solution was assessed through electrochemical polarization scanning and electrochemical impedance spectroscopy.

Findings revealed that coatings deposited with a spray mode comprising a 300 A current, 5.5 bar pneumatic pressure, and 160 mm standoff distance displayed higher Al and Mg elemental content compared to counterparts fabricated under different parameters. Porosity levels ranged from 7.38 to 11.82%, varying with spray mode. Over time, corrosion resistance varied due to the influence of corrosive products agglomerated on the coating surface. After 240 hours of immersion in 3.5 wt. % NaCl solution, microcracks emerged on the surface of coatings fabricated at 150A spray current, 4.0 bar spray pressure, and 100 mm spray distance, while no cracks were observed on others. XRD analysis indicated that the primary corrosion product on coating surfaces is predominantly Al (OH)3. The study inferred significant enhancement in corrosion mitigation attributed to elevated Al and Mg contents, surface homogeneity, and reduced porosity. Quantifying, characterizing, and minimizing coating porosity are essential for determining and improving the protective efficacy of coatings. Currently, numerous methods are under development for observing and measuring coating pores [14],[15],[17], including image analysis, mercury porosimetry, Brunauer-Emmett-Teller (BET) adsorption measurements, densitometry, high-resolution scanning electron microscopy, helium pycnometry, atomic force probes, contact measurement, ray-three-dimensional scanning imaging, and others.

Among these, the image analysis method, utilizing scanning electron microscope technology, stands out for its simplicity of operation and its ability to accurately quantify the number, shape, size, distribution, and other characteristics of pores. It has proven to be a reliable technique for pore analysis and has been endorsed by the International Organization for Standardization (ISO 26946) as the standard method for evaluating pores in thermal-sprayed coatings [14]. According to [15] utilized dimple grinding combined with optical microscopy to quantify internal porosity across the thickness of nine different electroless nickel-phosphorus (Ni-P) coatings deposited on Mg substrates. Additionally, scanning electron microscopy was employed to verify the identification of pores distinguished by dimpling. The influence of phosphorus (P) content within the Ni-P layers and the overall coating thickness on porosity was analyzed. Porosity reached its peak in coatings with high P content (10 wt% P) and was lowest in those with medium P content (5.2 wt% P). Furthermore, porosity exhibited a consistent decline with the augmentation of coating thickness, ranging from 28 μm to 57 μm. In a study investigating the effects of porosity and thermal gradients introduced during pulsed thermography, in [18] utilized pulsed thermography and a multilayer analytical model to critically assess the thermal diffusivity and inherent porosity in cold-sprayed Ti-6Al-4V coatings on Al6061-T6 substrates.

These coatings are crucial in utilizing cold spray as an additive manufacturing technique for the restoration of high-cost alloy components. The study drew upon experimental data obtained at spray angles ranging from 50◦ to 90◦, illustrating the relationship among the spray angle, porosity within the coating, and the resulting thermal diffusivity. The results revealed a decrease in porosity and an increase in thermal diffusivity as the spray angle increased from 50◦ to 90◦. Infrared thermography measurements of thermal diffusivity showed that the effective thermal diffusivity varied from 3.876% to 26.47% relative to the original coating thermal diffusivity when the spray angle decreased from 90◦ to 50◦. Correspondingly, numerical simulations performed on a partial representative microstructure of the coating illustrated a change ranging from 1.62% to 33.54% from the base coating thermal diffusivity. The analytical model, based on the effective medium theory using the Maxwell–Garnett approximation, forecasted a thermal alteration between 1.62% and 13.05% from the base coating thermal diffusivity. Microscopic analysis-based structural characterization revealed the variation in porosity content in cold spray coating with respect to the spray angle. It was found that the porosity percentage increased from 1.82% to 14.73% when the spray angle varied from 90◦ to 50◦. It was also observed that the porosity increased nonlinearly with the spray angle.

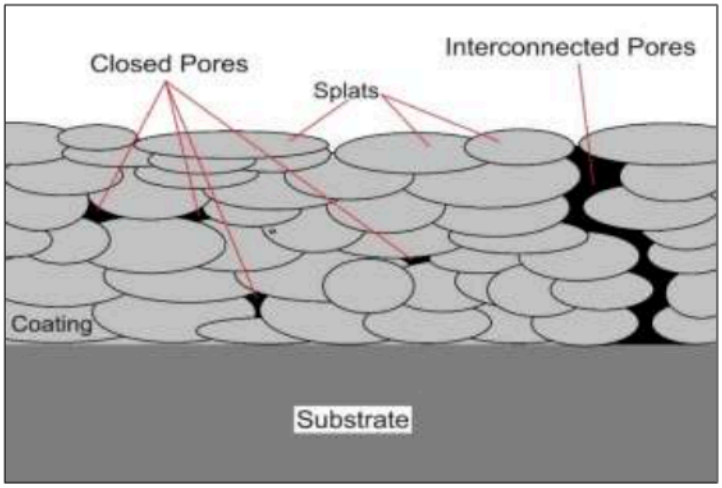

Figure 4: Schematic view of porosity in a thermal spray coating.
Source: Authors, (2026).

In a study investigating the adjustment of deposition parameters such as temperature, bias voltage, and pressure during magnetron sputtering to deposit Cr coatings with varying crystallographic orientations, crystallinity levels, and grain sizes, in [19] observed that during steam oxidation at 800 °C: Coatings deposited at 400 °C, with a bias voltage of –70 V, and at pressures ranging from 0.2 Pa to 0.5 Pa exhibited small grain sizes, high crystallinity, and random orientation. These characteristics contributed to favorable oxidation behavior, primarily due to their dense structure. Coatings deposited with a bias voltage range of 0 V to –40 V showed poor adhesion to the substrate, attributed to the low deposition energy of the plasma. Spallation of the oxide scale or metallic coating occurred during the oxidation test. Coatings deposited at 600 °C, with bias voltages ranging from –100 V to –200 V, and pressures between 2.0 Pa and 3.0 Pa, exhibited a strong (200) texture and large grain sizes. Intrinsic defects such as large grain boundaries and voids expanded into through-thickness cracks and large pores after oxidation. Coatings deposited at temperatures between 24 °C and 200 °C, at a pressure of 1.0 Pa, displayed slight texture and poor crystallinity. Oxygen-rich particles emerged in the un-oxidized coatings beneath the outer Cr2O3 layer after oxidation.

III.2.2 Microcracks

Variances in thermal gradients lead to the formation of cavities and micro-cracks, exacerbated by residual stresses, thermal expansion, and shrinkage during quenching cycles [8]. The roughness of coating surfaces, such as valleys, serves os stress concentration points, fostering crack initiation. Additionally, features like pores and splats in the coating's microstructure contribute to crack branching and deflect crack paths [20] (see Figure 5). The ceramic coating experiences heightened thermal gradient and residual stress due to differences in thermal expansion coefficients between adjacent layers, amplifying thermal mismatch stress within the coating system [21],[22]. In plasma-sprayed thermal barrier coatings (TBC), the bond coat/top coat (BC/TC) interface plays a crucial role due to the formation of the thermally grown oxide (TGO) layer and stress distribution at varying temperatures. Research shows that a smooth interface reduces stress, while rough interfaces increase stress during high-temperature exposure. Additionally, crack propagation mechanisms alter with interface roughness, with higher roughness promoting increased TBC fatigue life by spreading fatigue cracks along the interface and top coat, rather than concentrating them near the bond coat surface [23]. According to [23] devised a discrete element-based model to explore thermal stresses occurring at the interface between layers, attributed to the disparity in coefficients of thermal expansion (CTE).

Their findings suggest that the combination of CTE mismatch and thermally grown oxide (TGO) layer growth induces high tensile stress concentration within the bond coat (BC) layer upon cooling, leading to interface delamination. Conversely, stress reversal occurs in the thermal barrier coating (TC) layer, with increasing interface amplitude. The presence of porosity near crack propagation alters the crack path based on porosity orientation and shape. In regions without porosity, cracks converge to form larger branches, predominantly growing vertically within the ceramic TC. The TGO layer experiences compressive stresses, diminishing as the TC peak region is approached. A thicker TGO layer tends to generate a larger region of compressive stresses, potentially impeding crack propagation into and through the TC layer during the early cooling stages. The extended durability of thermal barrier coatings (TBC) faces a challenge from the infiltration and corrosion caused by calcium-magnesium-aluminum-silicate (CMAS). According to [24] investigated the microstructure and microcrack evolutions of CMAS-corroded TBCs through experiments and numerical modeling. In the study comparative experiments were conducted on TBCs that underwent treatment with and without CMAS at elevated temperatures for various durations.

Comparative experiments revealed that significant volume expansion, stemming from grain dissolution and TC corrosion due to CMAS, is the primary cause of TC spalling. Microcracks enriched with CMAS were observed at the TC/BC interface, resulting from a reaction between CMAS and TGO that degrades the interface. These microcracks act as pathways for CMAS infiltration, hastening the deterioration of CMAS-corroded TBCs. Additionally, the mechanism of microcrack evolution in CMAS-corroded TBCs is linked to the extent of CMAS coverage. When CMAS coverage is minimal, microcracks tend to propagate at the TC/BC interface and TC, leading to localized spalling. Conversely, greater CMAS coverage causes microcracks to extend solely at the TC/BC interface, resulting in the entire TC spalling. A coupled model has been developed, integrating CMAS penetration, TC corrosion and swelling, interfacial degradation, and microcrack propagation, providing insights into the degradation and failure process of CMAS-corroded TBCs as observed in the experiments. The laser surface melting technique, integrated into the deposition process, is renowned for enhancing the corrosion and erosion resistance of coatings. This method achieves heightened erosion resistance by compacting the surface layer. Laser glazing, while reducing surface roughness and enhancing microhardness, also leads to a slight increase in the coating's thermal diffusivity due to reduced surface porosity.

Moreover, laser glazing is effective in halting the spread of molten CMAS through the coating, thereby bolstering its resistance to hot corrosion. This enhancement is attributed to the formation of microcracks, which augment the strain tolerance of the topcoat [22],[25]. According to [25] conducted an analysis on the effects of laser modification post-coating deposition. This modification involves creating a pattern of through-thickness grooves within the coating, followed by surface layer remelting. Their findings concluded that the modified coating exhibited enhanced durability compared to the as-sprayed coating, reducing surface roughness from Sa 9.81 μm to Sa 0.75 μm. This reduction potentially leads to improved tribological flow conditions. Additionally, the modified coating showed an average 8.6 times increase in erosion resistance compared to as-sprayed coatings. This improvement can be attributed to surface densification and reduced influence of poor splat-to-splat adhesion in thermally sprayed coatings. Furthermore, there was an increase in CMAS resistance due to decreased propagation of molten silicates within the coating, along with an 11% enhancement in thermal fatigue resistance.

III.2.3 Unmelted Particles

In the thermal spraying process, uneven heating or irregular feedstock delivery can lead to inadequate melting of the spray particles. The utilization of larger-sized particles has been observed to decrease the temperature of the sprayed particles, resulting in a higher proportion of unmelted particles within the coating layer (shown in Figure 5).

This correlation associates the typical formation of pores in thermal spray processes with the presence of unmelted and semi-melted particles. These unmelted and partially melted droplets often demonstrate limited fluidity and formability, posing challenges in their ability to flatten and spread during deposition. Consequently, voids persist between the splats, which remain unfilled by the unmelted or semi-melted droplets even after the solidification of melted droplets [26, 27]. Unmelted particles represent a minority of the total incident particles (less than 10%), thus the occurrence of large pore formation is infrequent but significant [27]. As per Alebrahin et al. [28], unmelted particles may stem from the deposition of agglomerated submicron or nanosized particles, or from the impact of suspension droplets where not all the water evaporated during flight. The residual water evaporates on the hot substrate, leaving behind unmelted feedstock particles deposited on the substrate surface. In fact, the majority of individual submicron particles probably do not reach the substrate because of their low mass.

The varying sizes of unmelted particles are correlated with the atomization conditions within these spray parameters [29]. Significantly, coatings acquired through twin-wire arc spraying often showcase increased pore content owing to challenges in maintaining a consistent feed rate for feedstock wires compared to feedstock powders. Conversely, the HVOF spraying technique induces considerable plastic deformation of the splats during deposition due to the high particle velocity. Consequently, coatings produced through HVOF spraying typically exhibit dense, robust, and well-bonded characteristics [26]. In their investigation of unmelted particles in plasma spray, Ctibor et al. [30] revealed that typical unmelted particles are predominantly spheroidal and possess a microstructure closely linked to the powder fabrication process prior to spraying. These unmelted globular particles within the lamellar structure of the deposit tend to exhibit isotropic behavior under the influence of stress or other physical factors. Consequently, within the anisotropic structure of the coating, they act as centers of secondary defects, ultimately compromising the functional properties of the coatings.

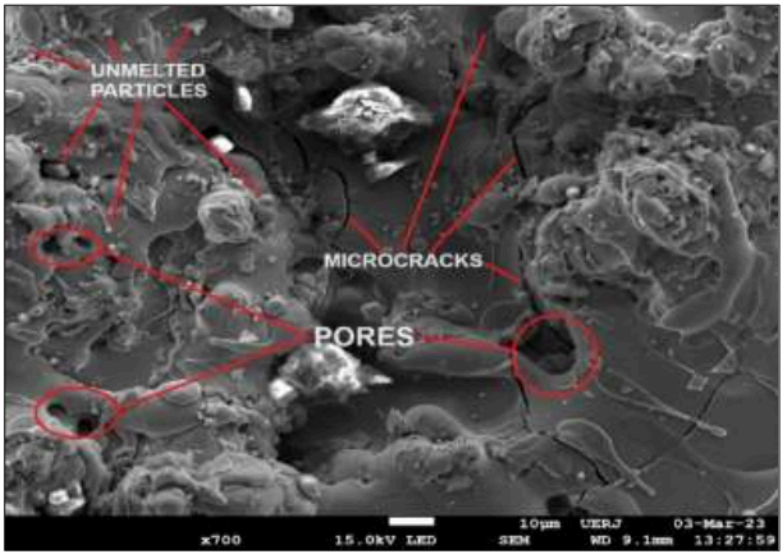

Figure 5: SEM micrograph presenting surface morphology and defects of a thermal sprayed coating.
Source: Authors, (2026).

III.2.4 Oxides

In the high-temperature spraying process, when particles meet the oxidizing atmosphere, they undergo oxidation. Reactive metals like aluminum, nickel, and chromium develop oxide layers during spraying, impacting both microstructure and coating bonding. These oxide layers limit the spread of molten particles upon impact, raising coating porosity and creating friction between the substrate and the splat [4],[26]. In their study, Brossard et al. [31] noted metal particle oxidation during spraying, manifesting in two forms: globular (enclosed within droplets) and as spinel on the outer surface. Subsequently, this oxidation process manifests as a ring-like granular structure within the spray coating. The researchers also attributed the oxidation of certain metals to high temperatures and low oxygen levels. Indeed, the occurrence of oxides in the coating is anticipated due to two factors. Firstly, molten particles are propelled under air pressure during projection. Secondly, each liquid alloy particle is enveloped by an air film during flight, leading to continued oxidation as oxygen becomes trapped upon impact with the target [32]. For metal coatings, a higher degree of oxidation typically corresponds to heightened porosity within the coating layer [25],[32]. Generally, oxidation levels can be reduced by utilizing inert gas, boosting the velocity of spray particles, or minimizing the distance between the spray gun and the substrate [31],[32]. During flame spraying, oxidation of spray particles is unavoidable since combustion requires a blend of oxygen and fuel gases.

Additionally, the oxide content of coatings produced by twin-wire arc spray might increase when compressed air is employed for droplet atomization and propulsion [30]. In HVOF spraying, the supersonic jet speeds up the spray particles, curbing oxide formation and yielding a coating with minimal oxide content. Further reduction in oxide content within HVOF-sprayed coatings can be achieved by lowering the temperature and boosting the velocity of spray particles [26]. According to [33] conducted a study on AlCoCrFeMo high entropy coatings (HECs) produced through three thermal spray techniques: low-pressure cold spray (LPCS), flame spray (FS), and high-velocity oxy-fuel spray (HVOF), aiming to create wear-resistant surfaces. The coatings were examined for their microstructures, phases, mechanical properties, and sliding wear behavior from room temperature up to 350°C. The LPCS, FS, and HVOF coatings initially exhibited a BCC solid solution phase. LPCS coatings lacked oxide inclusions, while FS and HVOF coatings displayed such inclusions due to in-flight oxidation (IFO). HVOF-sprayed coatings exhibited superior hardness due to their finer microstructure, reduced porosity, and fewer oxide inclusions compared to FS and LPCS coatings. The presence of oxide inclusions in FS and HVOF coatings contributed to increased hardness, while LPCS coatings had lower hardness and higher wear rates due to the absence of such inclusions. In terms of

tribological performance, LPCS coatings had lower frictional coefficients compared to FS and HVOF coatings at both tested temperatures. HVOF coatings showed improved wear resistance due to their higher hardness and the formation of a Co-based oxide film. Additionally, the presence of harder and stable Al- and Cr-based oxides provided protection against repetitive stresses during sliding.

III.3 QUANTIFICATION TECHNIQUES

Microstructural characterization plays a pivotal role in understanding and optimizing the performance of thermal spray coatings. These coatings often exhibit complex microstructures with a range of inherent imperfections, including voids, cracks, and unmelted or partially melted particles. Quantitative evaluation of geometrical features—most notably porosity—and detailed analysis of material aspects such as splat morphology, inter-splat interfaces, and phase composition are essential for correlating microstructural attributes with coating properties and in-service behavior. Among these features, porosity is particularly prevalent and has a critical impact on mechanical integrity, thermal conductivity, corrosion resistance, and other functional characteristics. As such, a variety of experimental techniques, including image analysis of cross-sectional micrographs, mercury intrusion porosimetry, and X-ray computed tomography, are commonly employed to measure and characterize porosity with high accuracy. The ability to reliably characterize these features is fundamental to the rational design and control of coating processes, enabling the production of coatings with predictable performance in demanding environments [34]. Nondestructive evaluation (NDE) techniques are widely employed for the detection and characterization of defects in materials and coatings, offering the advantage of preserving the structural integrity of the tested components. Common NDE methods include ultrasonic testing (UT), eddy current testing (ECT), X-ray radiography, and infrared thermography (IRT), among others.

Among these, ultrasonic testing (UT) has seen particularly rapid advancements in recent years, driven by improvements in sensor technology, signal processing, and imaging capabilities. These developments have significantly enhanced the resolution, sensitivity, and reliability of defect detection, making ultrasonic techniques increasingly suitable for the inspection of complex and multilayered coating systems [34]. When ultrasonic waves are transmitted into a sample via a coupling medium, internal defects disrupt their propagation by scattering or reflecting the acoustic energy, whereas regions without defects allow the ultrasound to propagate with minimal attenuation or distortion [34-37]. This contrast in wave behavior forms the basis for defect detection using ultrasonic testing. However, the effectiveness of this technique is limited in coatings with high porosity, as the numerous air-filled voids can scatter or absorb ultrasonic waves, thereby reducing signal clarity and measurement reliability [35-37]. Furthermore, the requirement for physical contact and the use of a coupling agent during measurement pose additional challenges when testing delicate or rough-coated surfaces [34]. Eddy current testing (ECT) operates on the principle of detecting variations in the amplitude and phase of eddy currents induced in a conductive material when subjected to alternating magnetic fields [34]. These eddy currents are influenced by the presence of defects, discontinuities, or changes in material properties, making ECT a valuable technique for surface and near-surface inspection.

However, the accuracy and sensitivity of ECT can be significantly affected by factors such as the electrical conductivity of the material, as well as the geometry, size, and shape of the test specimen. These dependencies necessitate careful calibration and consideration of material-specific parameters to ensure reliable defect detection [38], [39]. Infrared thermography (IRT) has emerged as a widely adopted technique for defect evaluation, owing to its non-contact nature, high efficiency, rapid data acquisition, and capacity for direct and quantitative characterization of subsurface anomalies [40],[41]. These advantages make IRT particularly attractive for real-time and large-area inspection applications. However, current limitations in spatial resolution and the relatively shallow penetration depth restrict its effectiveness for detecting deeply embedded defects. As a result, further research and technological development are required to enhance the resolution and subsurface imaging capabilities of infrared thermography, particularly for applications involving complex or multilayered materials [34]. A variety of experimental techniques are employed for the quantitative measurement and characterization of porosity in coatings, each with distinct advantages and limitations.

Water adsorption (WA) is a simple and cost-effective method; however, it exhibits limited sensitivity in distinguishing between samples with closely similar porosity levels. Mercury intrusion porosimetry (MIP) offers high precision in measuring open porosity but generally underestimates total porosity due to its inability to access closed pores. Helium pycnometry (HP) allows for the measurement of both open and closed porosity—provided the theoretical density of the material is known—but does not yield information on pore size or distribution. Image analysis (IA), commonly conducted on cross-sectional micrographs, enables the evaluation of both open and closed porosity, as well as pore size distribution and morphology. Nevertheless, the accuracy of IA is strongly influenced by spatial resolution and image contrast, and it lacks the ability to distinguish between open and closed pores. Electrochemical testing, although not capable of quantifying total porosity, provides valuable insight into pore connectivity within coatings. This method relies on the infiltration of an electrolyte through interconnected pores, leading to corrosion of the metallic substrate; higher connectivity results in increased corrosion current, offering an indirect measure of porosity interconnectivity [34], [42]. Small-angle neutron scattering (SANS) represents a more advanced technique, capable of resolving component porosities and providing surface area distributions associated with intrasplat cracks, interlamellar pores, and globular pores, including their approximate orientation.

These voids are commonly classified based on aspect ratios—1:1 for globular pores, 1:5 for interlamellar pores, and 1:10 for intrasplat cracks—enabling a more detailed and structural understanding of the coating's porosity network [43],[44]. The use of image processing (IP) techniques presents multiple advantages compared to conventional visual inspection, especially in the context of defect detection and quality control. IP offers enhanced precision and finer detail resolution, making it capable of identifying minor imperfections that may be overlooked by human inspectors. These systems can operate autonomously, significantly reducing the need for manual labor while enabling decisions to be made based on predefined rules and advanced algorithmic analysis. Additionally, IP ensures consistent and repeatable outcomes, which is valuable for tracking changes in defects over time. Remote inspection is another key benefit, as IP allows for the evaluation of areas that are difficult or dangerous to access, thereby increasing safety and eliminating the need for direct human presence. For high-volume production environments, IP is also more economical, lowering costs by increasing inspection throughput. Furthermore, IP systems rely on quantitative analysis, using detailed computations to assess defects and make objective judgments through sophisticated mathematical models. Collectively, these features highlight the clear benefits of IP over visual inspection in terms of reliability, efficiency, and safety [45-50].

According to [51] applied systematic image processing using ImageJ to analyze the microstructure of annealed environmental barrier coatings (EBCs), focusing on crack density, porosity, and phase distribution. Their results showed that REMS-rich coatings (M100 and M75D25) exhibited significant surface cracking (up to 0.58%), attributed to thermal expansion mismatch. In contrast, REDS-rich coatings (M25D75, M10D90, and D100) demonstrated improved microstructural stability, with lower crack coverage (0.04–0.14%) and porosity below 3%, highlighting the beneficial impact of REDS-rich compositions on coating integrity. In the study by [52], the effects of varying heat input on porosity, microstructure, microhardness, residual stress, and thermal behavior of martensitic stainless steel cladding on FGS600-3A ductile cast iron were investigated. Quantitative porosity analysis was performed using digital image processing with the NIS Elements-D software. The results demonstrated that heat input plays a critical role in pore and crack formation. As heat input increased, the porosity rose from 3.41% to 5.56%, with larger, more circular pores propagating between the first and second cladding layers. At lower heat inputs, pore formation was primarily attributed to lack of fusion, balling effect, and thermal contraction gradients.

III.4 ADDRESSING COATING DEFECTS THROUGH PREDICTIVE MACHINE LEARNING MODELS

Machine learning (ML) is a branch of artificial intelligence that enables computers to learn from data and improve their performance on tasks without being explicitly programmed. It involves the use of various algorithms designed to analyze data, identify patterns, and make decisions or predictions. The choice of algorithm depends on factors such as the nature of the problem, the type and number of variables involved, and the most suitable model for the task. ML enhances data handling efficiency and is widely applied across domains to solve complex data-driven problems [53]. Machine learning, is known for its low computational cost and rapid development cycle, is increasingly being applied in material science due to its powerful data processing capabilities and high predictive accuracy. It plays a key role in material detection, analysis, and design, and has been successfully used to discover new materials, predict molecular and material properties, study quantum chemistry, and aid in drug design.

By significantly reducing the need for costly density functional theory (DFT) calculations and repetitive laboratory experiments, machine learning offers an efficient alternative for accelerating scientific discovery [53],[54]. Conventionally, the Taguchi design method has been widely used to identify optimal process parameters and differentiate between major and minor factors influencing coating properties. However, its effectiveness diminishes when complex interactions among numerous parameters affect coating quality [55]. Machine learning (ML) techniques address these limitations by capturing nonlinear relationships and intricate dependencies. Among these, artificial neural networks (ANNs), with their flexible architectures and strong learning capabilities, are particularly effective for predicting and optimizing thermal spraying processes [56]. Artificial Neural Networks (ANNs) are computational models inspired by the structure and function of the human brain. Composed of interconnected artificial neurons organized in layers—typically including an input layer, one or more hidden layers, and an output layer—ANNs are capable of recognizing complex, nonlinear patterns in data.

Each neuron processes input signals by computing a weighted sum, applying an activation function, and producing an output. The weights, analogous to synapses in biological systems, are adjusted through training, allowing ANNs to learn from data and make predictions or classifications. This adaptive learning capability makes ANNs particularly effective in solving intricate problems, such as optimizing conditions in manufacturing processes [55], [57]. In the context of thermal spray processes, artificial neural networks (ANNs) offer a powerful solution for modeling the intricate chemical and thermodynamic reactions that drive coating formation. Given the challenge of acquiring large datasets in this field, shallow ANNs—comprising fewer than three hidden layers—have become a practical choice for effective prediction and analysis in data-scarce scenarios [55]. In a study by [55], an ANN-based regression model was developed to predict key coating properties—such as thickness, porosity, and erosion slurry resistance—based on process parameters like oxygen (O), LPG (L), and air flow (A) rates. Optimized with a single hidden layer of 20 neurons, the model showed strong agreement with experimental results, with validation through SEM imaging, porosity analysis, and mass loss measurements confirming its predictive accuracy. The Backpropagation (BP) neural network is a widely used training algorithm that minimizes prediction error by iteratively adjusting the network's weights and thresholds.

It consists of an input layer, hidden layer(s), and an output layer, operating through forward propagation of signals and backward propagation of errors. In forward propagation, input data undergoes nonlinear transformation through the network to generate an output. If a discrepancy exists between the predicted and actual output, the error is propagated backward to update weights accordingly. To ensure data validity and model effectiveness, input and output features must be preprocessed—commonly through normalization—before training. Through repeated learning, the network converges on weight values that minimize prediction error [58],[59]. The genetic algorithm (GA) is an optimization technique inspired by natural evolution, simulating processes such as gene crossover and mutation to search for optimal solutions. It is particularly effective for solving complex combinatorial problems, often outperforming traditional optimization methods [58]. In the context of BP neural networks, GA can be used to optimize initial weights and thresholds, addressing the variability and instability that arise when these parameters are randomly assigned [58], [60]. The GA-BP neural network combines the strengths of genetic algorithms and backpropagation, offering significant advantages in parameter optimization. By automatically adjusting the network structure and parameters without the need for pre-experiments, this hybrid method enhances the model's generalization ability and improves prediction accuracy [61].

In a study by [61], a 3D transient model combining computational fluid dynamics and surface reaction modeling was developed to analyze flame flow and particle oxidation during the HVOF WC-12Co thermal spraying process. The results revealed that oxide layer thickness varies significantly with particle size, from about 90 Å for 5 μm particles to just 8 Å for 60 μm particles. Using a GA-BP neural network, the researchers optimized key parameters—particle size, oxygen/fuel ratio, and nitrogen flow rate—identifying ideal values for improved coating performance. Experimental validation confirmed that the optimized coating exhibited fewer defects, lower oxide content, and enhanced hardness and wear resistance. Convolutional Neural Networks (CNNs) are a type of feedforward neural network designed to automatically extract meaningful features from raw data using convolutional structures. Inspired by the human visual system, CNNs eliminate the need for manual feature extraction by learning hierarchical patterns directly from the data. They are particularly effective in tasks involving local interactions, such as image recognition and computational materials science.

Key architectural advantages include local connections, which limit each neuron's input to a small region, reducing computational complexity; weight sharing, which minimizes the number of trainable parameters and improves generalization; and pooling layers, which downsample feature maps to retain essential information while discarding redundancy. These features make CNNs efficient, scalable, and well-suited for a wide range of pattern recognition problems [62],[63]. According to [64] developed a deep ensemble convolutional neural network trained on 500 scanning electron microscopy (SEM) images, achieving a test accuracy of 96.0%. Their model demonstrated strong performance across all evaluation metrics, with training, validation, and test accuracies reaching 94.7%, 100%, and 96.0%, respectively. The classification system was particularly effective at distinguishing between different wear patterns, with only minimal confusion between similar mechanisms, resulting in just 4 misclassifications out of 100. This study highlighted how integrating deep learning with materials science can provide a scalable and efficient methodology for tribological analysis and material design.

Physics-Informed Neural Networks (PINNs) are a hybrid machine learning approach that integrates physical laws, typically expressed as partial differential equations (PDEs), directly into the training process of neural networks. By embedding these equations into the loss function through automatic differentiation, PINNs guide the model to produce solutions that are both consistent with the data and compliant with the governing physics of the system. This approach addresses the limitations of traditional machine learning models, such as ANNs and CNNs, which often struggle to generalize to unfamiliar structures. In thermal fluid studies, for example, PINNs have been successfully applied to solve momentum and energy transport equations, accurately predicting particle velocity and temperature. Designed specifically to incorporate any underlying physical law described by nonlinear PDEs, PINNs are especially effective in scenarios with limited data, leveraging known physical principles to enhance model accuracy and reliability [63], [65].

According to [63] developed a hierarchical neural network combining Physics-Informed Neural Networks (PINNs) and Convolutional Neural Networks (CNNs) to predict in-flight particle properties and the performance of NiCr–Cr_3C_2 coatings, including porosity, microhardness, and wear rate. Using a random forest model, they identified spraying distance and particle velocity as the most influential parameters. Their approach achieved prediction accuracies of up to 99%, providing a strong foundation for the development of intelligent HVOF spraying systems. In thermal spray processes, machine learning (ML) offers a powerful way to model complex chemical and thermodynamic reactions. However, limited data availability and the unexplored influence of input variables in ML models present significant challenges.

V. CONCLUSIONS

Thermal spray coatings find widespread application in the fabrication of gas turbine engines, internal combustion engines, bearings, pumping systems, compressor and pipeline equipment, as well as medical implant materials. This technique encompasses a range of cost-effective and dependable methods aimed at safeguarding, repairing, and rejuvenating components, thereby prolonging their operational lifespan even in harsh environments. Defects are inherent in these coatings, emerging from compositional imbalances resulting from metallurgical changes within the structures or irregular surface morphology arising from the layer-by-layer deposition and fusion process on material surfaces. These surface irregularities serve as sites for stress concentration, facilitating crack formation. The presence and nature of defects are greatly influenced by both the feedstock materials and the parameters of the deposition process. Non-dense crystallographic orientation, poor accumulation of large grains, and irregular atomic arrangement in amorphous regions are all detrimental to the compactness of the coatings and negatively affect their oxidation behavior. Although defects are characteristic of thermal spray coatings, machine learning presents a valuable opportunity to advance the control and optimization of thermal spray coatings by modeling the complex chemical and thermodynamic interactions that influence coating quality. Despite the challenges posed by limited data and the underexplored impact of individual process variables, ML enables more accurate prediction of defect formation and supports the development of optimized spraying parameters. As a result, it offers a powerful tool for improving coating performance, reducing defects, and extending the service life of components in demanding environments.

VI. AUTHOR'S CONTRIBUTION

Conceptualization: Uirá Montani, Marília Garcia Diniz, Paolo Bettini, Hector Reynaldo Meneses Costa.
Methodology: Uirá Montani, Hector Reynaldo Meneses Costa.
Investigation: Uirá Montani.
Discussion of results: Uirá Montani, Hector Reynaldo Meneses Costa.
Writing – Original Draft: Uirá Montani.
Writing – Review and Editing: Uirá Montani, Marília Garcia Diniz, Hector Reynaldo Meneses Costa.
Resources: Uirá Montani, Marília Garcia Diniz, Paolo Bettini, Hector Reynaldo Meneses Costa.
Supervision: Marília Garcia Diniz, Hector Reynaldo Meneses Costa.
Approval of the final text: Uirá Montani, Marília Garcia Diniz, Paolo Bettini, Hector Reynaldo Meneses Costa.

VII. DECLARATIONS

Data Availability: The data that support the findings of this study are available from the corresponding author upon reasonable request.
Competing Interests: The authors declare that they have no conflict of interest.
Declaration of generative AI and AI-assisted technologies in the writing process: During the preparation of this work, the authors used Chat-GPT in order to improve the readability and language. After using this tool/service, the authors reviewed and edited the content as needed and take full responsibility for the content of the publication.

VIII. REFERENCES

[1] Sathish, M.; Radhika, N.; Saleh, Bassiouny. Duplex and composite coatings: a thematic review on thermal spray techniques and applications. Metals and Materials International, v. 29, n. 5, p. 1229-1297, 2023.

[2] Singh, Surinder et al. Applications and developments of thermal spray coatings for the iron and steel industry. Materials, v. 16, n. 2, p. 516, 2023.

[3] Zhang, Panpan et al. Microstructures and Wear Resistance of Mo Coating Fabricated by In Situ Laser-Assisted Plasma Spraying. Journal of Thermal Spray Technology, p. 1-13, 2023.

[4] Qadir, Danial et al. A review on coatings through thermal spraying. Chemical Papers, v. 78, n. 1, p. 71-91, 2024.

[5] RigamontI, Daniela et al. Thermal spray to embed optical fibers for the monitoring and protection of metallic structures. Journal of Materials Science, v. 59, n. 27, p. 12812-12829, 2024.

[6] Du, Xinwei et al. Wire arc additive manufacturing from the perspective of remanufacturing: A review of data processing. Journal of Manufacturing Processes, v. 107, p. 385-410, 2023.

[7] Palumbo, Joshua; Chandra, Sanjeev. Additive manufacturing of complex structures and flow channels using wire-arc thermal spray. Journal of Manufacturing Processes, v. 107, p. 459-471, 2023.

[8] Mohanty, Shalini; Gokuldoss Prashanth, Konda. Metallic coatings through additive manufacturing: A review. Materials, v. 16, n. 6, p. 2325, 2023.

[9] Senol, Seren et al. Improved surface quality and fatigue life of high-strength, hybrid particle reinforced (Ti+ B4C)/Al-Cu-Mg metal matrix composite processed by dual-laser powder bed fusion. Procedia Structural Integrity, v. 53, p. 12-28, 2024.

[10] Maleki, Erfan; Bagherifard, Sara; Guagliano, Mario. Correlation of residual stress, hardness and surface roughness with crack initiation and fatigue strength of surface treated additive manufactured AlSi10Mg: Experimental and machine learning approaches. Journal of Materials Research and Technology, v. 24, p. 3265-3283, 2023.

[11] Vaz, Rodolpho F. et al. Cavitation resistance of FeMnCrSi coatings processed by different thermal spray processes. Hybrid Advances, v. 5, p. 100125, 2024.

[12] Arshid, Ehsan; Amir, Saeed; Loghman, Abbas. On the vibrations of FG GNPs-RPN annular plates with piezoelectric/metallic coatings on Kerr elastic substrate considering size dependency and surface stress effects. Acta Mechanica, v. 234, n. 9, p. 4035-4076, 2023.

[13] Nguyen, Tuan-Linh et al. Analysis of the effect of spray mode on coating porosity and hardness when spraying press screws by the high velocity oxy fuel method. EUREKA: Physics and Engineering, n. 6, p. 93-103, 2023.

[14] Li, Bo et al. Study on Porosity of Thermal-Sprayed Commercially Pure Aluminum Coating. Materials, v. 16, n. 19, p. 6612, 2023.

[15] Hu, H. et al. Dimple Grinding Coupled with Optical Microscopy for Porosity Analysis of Metallic Coatings. Micron, v. 178, p. 103593, 2024.

[16] Nguyen, Tuan Van et al. Characterization and corrosion resistance of the twin-wire Arc spray Al-5Mg alloy coating applied on a carbon steel substrate. Journal of Thermal Spray Technology, p. 1-17, 2023.

[17] De Formanoir, Charlotte et al. Healing of keyhole porosity by means of defocused laser beam remelting: Operando observation by X-ray imaging and acoustic emission-based detection. Additive Manufacturing, v. 79, p. 103880, 2024.

[18] Unnikrishnakurup, Sreedhar et al. Exploring thermal dynamics and porosity of cold-sprayed Ti-6Al-4V coatings on Al6061-T6 substrates: A pulsed thermography and numerical modeling approach. International Journal of Thermal Sciences, v. 196, p. 108732, 2024.

[19] Meng, Yan et al. Effect of deposition parameters on characteristics and oxidation behavior of magnetron sputtered Cr coatings. Journal of Nuclear Materials, v. 588, p. 154802, 2024.

[20] Amer, Mohamed et al. Unraveling the Cracking Mechanisms of Air Plasma-Sprayed Thermal Barrier Coatings: An In-Situ SEM Investigation. Coatings, v. 13, n. 9, p. 1493, 2023.

[21] Tao, Shiqian et al. Effect of Cracks on Thermal Shock Behavior of Plasma-Sprayed Thick Thermal Barrier Coatings. Journal of Materials Engineering and Performance, v. 32, n. 11, p. 4998-5014, 2023.

[22] Sokolowski, Pawel et al. The behavior of plasma sprayed thermal barrier coating with laser microtextured bond coat under high temperature testing. Surface and Coatings Technology, v. 453, p. 129095, 2023.

[23] Ferguen, N.; Leclerc, W.; Lamini, E.-S. Numerical investigation of thermal stresses induced interface delamination in plasma-sprayed thermal barrier coatings. Surface and Coatings Technology, v. 461, p. 129449, 2023.

[24] Zhou, Qianqian et al. Microstructure and microcrack evolution mechanism of thermal barrier coatings under CMAS infiltration and corrosion: Experimental and numerical modeling. Corrosion Science, v. 229, p. 111890, 2024.

[25] Ushmaev, Dmitrii; Norton, Andy; Kell, James. Thermally sprayed coatings resistant to environmental degradation: Columnar-like coatings through laser ablation and surface melting approach. Surface and Coatings Technology, v. 460, p. 129394, 2023.

[26] Chen, Tai-Cheng et al. The influence of coating microstructure on the corrosion behavior of Inconel 625 coatings fabricated through different thermal spraying processes. Surface and Coatings Technology, p. 130674, 2024.

[27] De Oca Zapiain, David Montes et al. Calibration of thermal spray microstructure simulations using Bayesian optimization. Computational Materials Science, v. 235, p. 112845, 2024.

[28] Alebrahim, Elnaz et al. Tailoring the porosity level of the suspension plasma sprayed coatings using a dual suspension injection system. Surface and Coatings Technology, v. 478, p. 130401, 2024.

[29] Taghi-Ramezani, Saeid; Valefi, Zia. Effects of Spray Parameters on the YSZ-Alumina Splat Formation During Solution Precursor High Velocity Flame Spraying. Metals and Materials International, p. 1-13, 2023.

[30] ctibor, pavel; roussel, olivier; tricoire, Aurelien. Unmelted particles in plasma sprayed coatings. Journal of the European Ceramic Society, v. 23, n. 16, p. 2993-2999, 2003.

[31] Brossard, S. et al. Study of the microstructure of NiCr splats plasma sprayed on to stainless steel substrates by TEM. Surface and Coatings Technology, v. 204, n. 9-10, p. 1608-1615, 2010.

[32] Boudjit, Sarra et al. Mechanical, Tribological, and Electrochemical Evaluation of NiCrAlMoFe Thermally Sprayed Coatings Subject to Post-treatments. Journal of Materials Engineering and Performance, p. 1-14, 2024.

[33] Patel, Payank et al. Enhanced wear resistance of AlCoCrFeMo high entropy coatings (HECs) through various thermal spray techniques. Surface and Coatings Technology, v. 477, p. 130311, 2024.

[34] Deshpande, Swarnima et al. Application of image analysis for characterization of porosity in thermal spray coatings and correlation with small angle neutron scattering. Surface and Coatings Technology, v. 187, n. 1, p. 6-16, 2004.

[35] Lemlikchi, Safia et al. Ultrasonic characterization of thermally sprayed coatings. Journal of Thermal Spray Technology, v. 28, p. 391-404, 2019.

[36] Meng, Jiajian et al. Mechanical properties measurement of chromium coatings based on laser ultrasonic technology in high-temperature conditions. Mechanical Systems and Signal Processing, v. 228, p. 112421, 2025.

[37] Zawischa, Martin; Makowski, Stefan; Toma, Filofteia-Laura. Fast and Nondestructive Mechanical Characterization of Thermally Sprayed and Laser Cladded Coatings: Automated Surface Acoustic Wave Spectroscopy as a New Tool for Quality Control and Research. Journal of Thermal Spray Technology, v. 34, n. 2, p. 928-938, 2025.
[38] He, Dongfeng; Kusano, Masahiro; Watanabe, Makoto. Detecting the defects of warm-sprayed Ti-6Al-4V coating using Eddy current testing method. Ndt & E International, v. 125, p. 102565, 2022.

[39] Tytko, Grzegorz et al. High frequency eddy current method in inspection of aluminide coatings integrity after simulating service loads. Measurement, v. 252, p. 117356, 2025.

[40] Wei, Jinfeng et al. Quantitative characterization of interfacial defects in thermal barrier coatings by long pulse thermography. Coatings, v. 12, n. 12, p. 1829, 2022.

[41] CernuschI, Federico; Bison, Paolo. Thirty Years of Thermal Barrier Coatings (TBC), Photothermal and thermographic techniques: Best practices and lessons learned. Journal of Thermal Spray Technology, v. 31, n. 4, p. 716-744, 2022.

[42] Andreola, Fernanda; Leonelli, Cristina; Romagnoli, Marcello. Techniques Used to Determine Porosity. American Ceramic Society Bulletin, v. 79, n. 7, p. 49-52, 2000.

[43] Allen, Andrew J. et al. Microstructural characterization of yttria-stabilized zirconia plasma-sprayed deposits using multiple small-angle neutron scattering. Acta Materialia, v. 49, n. 9, p. 1661-1675, 2001.

[44] Kulkarni, A. et al. Comprehensive microstructural characterization and predictive property modeling of plasma-sprayed zirconia coatings. Acta Materialia, v. 51, n. 9, p. 2457-2475, 2003.

[45] Mehrali, Hossein et al. Detection of coating defects in high gas turbine blades by image processing. Signal, Image and Video Processing, v. 19, n. 5, p. 360, 2025.

[46] Deng, Liwei; Guo, Yangang; Chai, Borong. Defect detection on a wind turbine blade based on digital image processing. Processes, v. 9, n. 8, p. 1452, 2021.

[47] Aust, Jonas et al. Automated defect detection and decision-support in gas turbine blade inspection. Aerospace, v. 8, n. 2, p. 30, 2021.

[48] Rizk, Patrick et al. Wind turbine blade defect detection using hyperspectral imaging. Remote Sensing Applications: Society and Environment, v. 22, p. 100522, 2021.

[49] Aminzadeh, Ahmad et al. Non-contact inspection methods for wind turbine blade maintenance: techno–economic review of techniques for integration with industry 4.0. Journal of Nondestructive Evaluation, v. 42, n. 2, p. 54, 2023.

[50] Rao, Yizhuo et al. Wind turbine blade inspection based on unmanned aerial vehicle (UAV) visual systems. In: 2019 IEEE 3rd conference on energy internet and energy system integration (EI2). ieee, 2019. p. 708-713.

[51] Wang, Keyu et al. An in-depth exploration of microstructural characteristics and phase evolution in RE-silicates (RE= Er0. 25Tm0. 25Yb0. 25Lu0. 25) multiphase environmental barrier coatings utilizing digital image processing techniques. Journal of the European Ceramic Society, p. 117276, 2025.

[52] Altay, Meryem; aydin, hakan; karşi, adem. effect of heat input on martensitic stainless-steel laser clad characteristics on ductile cast iron. welding in the world, p. 1-17, 2025.

[53] Mahesh, Batta et al. Machine learning algorithms-a review. International Journal of Science and Research (IJSR). [Internet], v. 9, n. 1, p. 381-386, 2020.

[54] Wei, Jing et al. Machine learning in materials science. InfoMat, v. 1, n. 3, p. 338-358, 2019.

[55] Singh, Vikrant et al. Predictive modeling of HVOF-sprayed TiC coating: an ANN-based approach for coating properties estimation. International Journal on Interactive Design and Manufacturing (IJIDeM), v. 19, n. 3, p. 1709-1720, 2025.

[56] Gui, Longen et al. Prediction of in-flight particle properties and mechanical performances of HVOF-sprayed NiCr–Cr3C2 coatings based on a hierarchical neural network. Materials, v. 16, n. 18, p. 6279, 2023.

[57] Kumar, Suresh S. et al. Numerical analysis of thermal spray coatings using artificial neural networks (ANN) overview. International Journal on Interactive Design and Manufacturing (IJIDeM), p. 1-16, 2024.

[58] Ye, Dongdong et al. Prediction and analysis of the grit blasting process on the corrosion resistance of thermal spray coatings using a hybrid artificial neural network. Coatings, v. 11, n. 11, p. 1274, 2021.

[59] Zhou, Kai et al. Fault diagnosis of spraying workshop based on BP neural network. In: Journal of Physics: Conference Series. IOP Publishing, 2021. p. 032074.

[60] JIang, Qin et al. Application of BP neural network based on genetic algorithm optimization in evaluation of power grid investment risk. IEEE Access, v. 7, p. 154827-154835, 2019.

[61] Li, Siyu et al. Evaluation and Analysis of Particle Oxidation of HVOF Thermal Spraying Based on GA-BP Neural Network Algorithm. Journal of Thermal Spray Technology, p. 1-24, 2025.

[62] Li, Zewen et al. A survey of convolutional neural networks: analysis, applications, and prospects. IEEE transactions on neural networks and learning systems, v. 33, n. 12, p. 6999-7019, 2021.

[63] Gui, Longen et al. Prediction of in-flight particle properties and mechanical performances of HVOF-sprayed NiCr–Cr3C2 coatings based on a hierarchical neural network. Materials, v. 16, n. 18, p. 6279, 2023.

[64] Paprk, Tae-Jun et al. Deep Learning-Enhanced Wear Analysis of Fe-Cr Composite Coatings for Automotive Brake Applications Under Euro 7 Requirements. Sahn and Oh, Yoon-Suk, Deep Learning-Enhanced Wear Analysis of Fe-Cr Composite Coatings for Automotive Brake Applications Under Euro, v. 7, 2025.

[65] Bobzin, K.; Heinemann, H.; Dokhanchi, A. Physics-Informed Neural Networks for Predicting Particle Properties in Plasma Spraying. In: International Thermal Spray Conference. ASM International, 2024. p. 452-458.